Organic Electronics 13 (2012) 1197–1203

Contents lists available at SciVerse ScienceDirect

Organic Electronics

journal homepage: www.elsevier.com/locate/orgel

Anthracene derivatives as efficient emitting hosts for blue organic light-emitting diodes utilizing triplet–triplet annihilation

Hirohiko Fukagawa [a,*], Takahisa Shimizu [a], Noriyuki Ohbe [b], Shizuo Tokito [a,1], Katsumi Tokumaru [c], Hideo Fujikake [a]

[a] Japan Broadcasting Corporation (NHK), Science and Technology Research Laboratories, 1-10-11 Kinuta, Setagaya-ku, Tokyo 157-8510, Japan
[b] Tokyo University of Science, 1–3 Kagurazaka, Tokyo 162-8610, Japan
[c] University of Tsukuba, 1-1-1 Tennodai, Tsukuba, Ibaraki 305-8577, Japan

ARTICLE INFO

Article history:
Received 20 October 2011
Received in revised form 20 February 2012
Accepted 11 March 2012
Available online 6 April 2012

Keywords:
Blue organic light-emitting diode
Anthracene
Triplet–triplet annihilation

ABSTRACT

The molecular design strategies for the host materials suitable for highly efficient, blue fluorescent organic light-emitting diodes (OLEDs) are demonstrated. The device characteristics of blue fluorescent OLEDs are compared with different host materials. Some devices exhibit a highly efficient blue electroluminescence with a high external quantum efficiency of more than 7%. The correlation between OLED efficiency and triplet–triplet annihilation is characterized by measuring the up-conversion of triplet excited states into singlet ones. The host materials require an anthracene unit and a bulky molecular structure to prevent the overlap of anthracene units between adjacent molecules in the film.

1. Introduction

Much interest has been focused on organic light-emitting diodes (OLEDs) because of their potential applications in full-color large displays and lighting applications. Red, green, and blue emissions in OLEDs that are highly efficient and have long device lifetimes and high color purity are important for device applications. There have been many reports on high-performance red and green OLEDs [1–7]. However, the performance of blue OLEDs has been relatively poor compared with those of the red and green ones, and thus it is necessary to improve their performance. Blue fluorescent OLEDs tend to have longer lifetimes and higher color purities than blue phosphorescent OLEDs [7,8]. However, the internal quantum efficiency (η_{int}) of conventional fluorescent OLEDs is limited to 25% since the singlet and triplet excitons are generated at a ratio of about 1:3 under electrical excitation. The key to improving the efficiency of fluorescent OLEDs is the use of triplet excitons.

Two possible mechanisms for the up-conversion of a triplet excited state (T_1) into a singlet excited state (S_1) have already been proposed. One possible up-conversion mechanism is triplet–triplet annihilation (TTA, i.e., *p*-type delayed fluorescence) [9] and the other is thermally activated delayed fluorescence (TADF, i.e., E-type delayed fluorescence) [10]. In the TTA process, S_1 or T_1 arises from the reaction between two T_1. This additional singlet exciton production can increase the efficiency by 15% to 37.5% depending on the up-conversion mechanism [11–14]. Thus, the maximum η_{int} can be increased by up to 40% or 62.5%. Although a maximum η_{int} of 100% is favorable via the TADF process, it remains difficult to develop an efficient blue OLED owing to the lack of a suitable wide-gap material [15–17]. There have been several reports on efficient blue fluorescent OLEDs utilizing TTA, where anthracene derivatives are used as host materials [13,14]. Thus, it is assumed that anthracene is the key unit to realizing highly efficient blue fluorescent OLEDs. Anthracene derivatives exhibit relatively high photoluminescence (PL) [18], electroluminescence (EL), and electrochemical properties.

* Corresponding author. Tel.: +81 3 5494 3254; fax: +81 3 5494 3297.
E-mail address: fukagawa.h-fe@nhk.or.jp (H. Fukagawa).
[1] Present address: Yamagata University, 4-3-16 Jonan, Yonezawa, Yamagata 992-8510, Japan.

1566-1199/$ - see front matter © 2012 Elsevier B.V. All rights reserved.
http://dx.doi.org/10.1016/j.orgel.2012.03.019

The main problem in their use is their thermal stability due to the high crystallinity of the anthracene unit. Several anthracene derivatives with a high glass transition temperature (T_g) have been synthesized and used to develop efficient blue OLEDs [19,20]. However, the origin of the high efficiency in such blue OLEDs was proposed to be only the efficient energy transfer from the anthracene derivative host to the fluorescent guest [20]. The relationship between the molecular structure of the anthracene derivatives and the TTA process in the efficient blue OLEDs has never been clarified.

In this work, we report the molecular design strategies for an anthracene derivative for developing highly efficient blue OLEDs utilizing TTA. The device characteristics of four types of blue fluorescent OLEDs, the emitting layers of which consist of different hosts and a blue fluorescent dopant 4,4′-bis[4-(diphenylamino)styryl]biphenyl (BDAVBi), are compared. Two of the anthracene derivatives we used as hosts are 2,2′-bis(anthracen-9-yl)-9,9′-spirobifluorene (Spiro-FA) and 2,2′-bis(10-phenylanthracen-9-yl)-9,9′-spirobifluorene (Spiro-FPA) [21]. They slightly differ in molecular structure, as shown in Fig. 1. The third anthracene derivative we used as a host is a pure blue-emitting material, 2-methyl-9,10-bis(naphthalen-2-yl)anthracene (MADN) [8,19]. The last host material is not an anthracene derivative, 4,4′-bis(2,2′-diphenyl-vinyl)-1,1′-biphenyl (DPVBi), which is well-known as a highly efficient blue-emitting material. The OLEDs using Spiro-FPA and MADN have a maximum external quantum efficiency (η_{ext}) of more than 7%, whereas the other two OLEDs have a maximum η_{ext} of about 5%. The anthracene unit is found to be significantly important for realizing efficient blue OLEDs utilizing TTA by measuring the transient decay of the electroluminescence of OLEDs. In addition, by examining the differences in the device characteristics of the OLED using Spiro-FPA and the OLED using Spiro-FA, we have clarified the requirements for the host material for developing highly efficient blue OLEDs.

2. Experimental

The OLEDs were developed on a glass substrate coated with a 150-nm-thick indium-tin-oxide (ITO) layer. Prior to the fabrication of the organic layers, the substrate was cleaned with ultra purified water and organic solvents, and treated with a UV–ozone ambient. The organic layers were sequentially deposited onto the substrate without breaking the vacuum at a pressure of about 10^{-5} Pa. We fabricated blue OLEDs with a structure ITO(150 nm)/m-MTDATA (15 nm)/α-NPD (55 nm)/host:BDAVBi (3 wt% doped, 30 nm)/Alq_3 (40 nm)/lithium fluoride (1.0 nm)/alu-

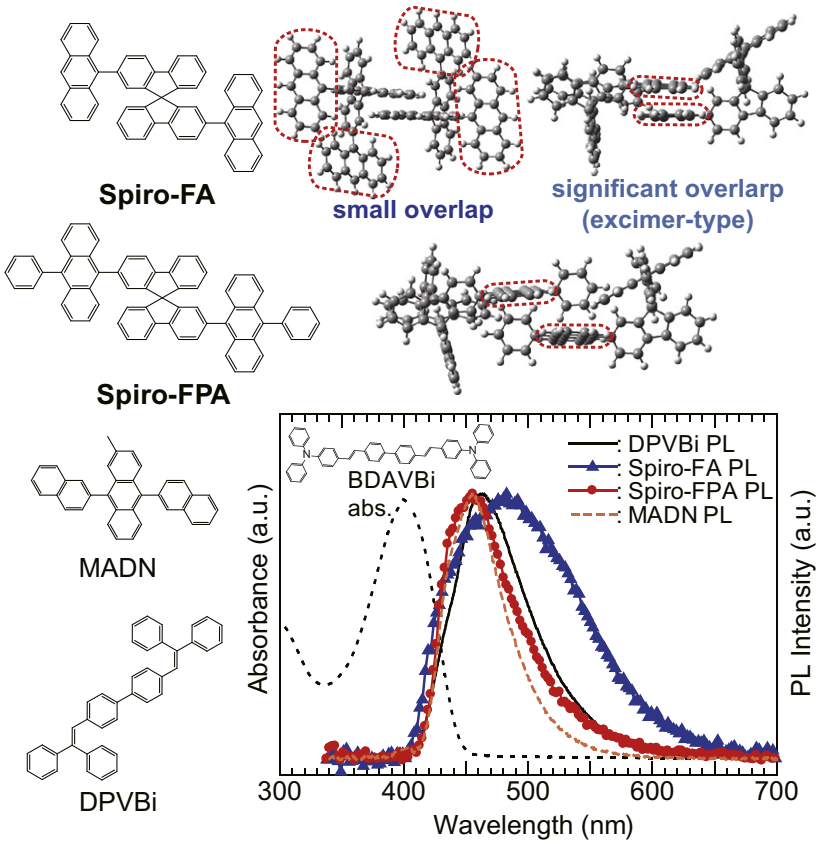

Fig. 1. Optical absorption spectrum of BDAVBi in dilute toluene solution and PL spectra of DPVBi, Spiro-FA, Spiro-FPA, and MADN thin films. The optical geometries at the B3LYP/6-31G (d, p) level and the examples of the molecular packing structure of two adjacent molecules of Spiro-FA and Spiro-FPA are also shown.

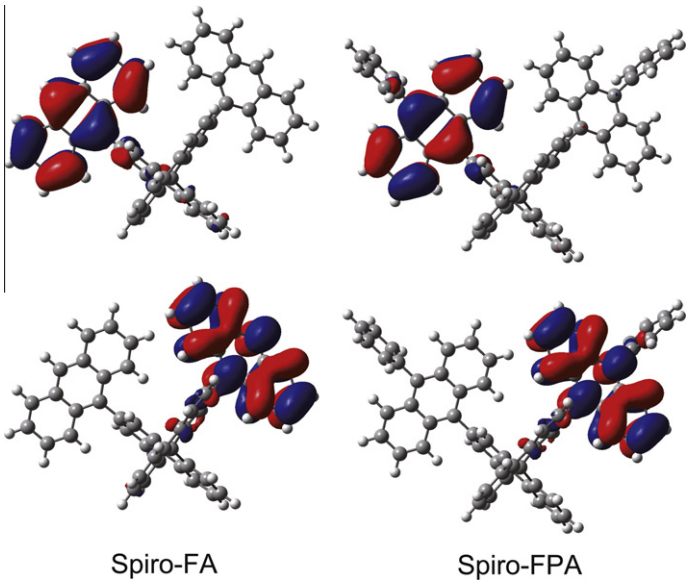

Fig. 2. Calculated HOMO (top) and LUMO (down) density maps of Spiro-FA and Spiro-FPA at B3LYP/6-31G (d, p) level.

minum (100 nm) (where ITO is indium tin oxide, m-MTDATA is 4,4′,4″-tris-(3-methyl-phenylphenylamino)triphenylamine, α-NPD is *N*,*N*′-di(naphthalen-1-yl)-*N*,*N*′-diphenylbenzidine, and Alq_3 is tris(8-quinolinolato)-aluminum). The devices were encapsulated using UV-epoxy resin and a glass cover within a nitrogen atmosphere after cathode formation. A spectroradiometer (Minolta CS-1000) was used to measure the EL spectra and luminance. A digital source meter (Keithley 2400) and a desktop computer were used to operate the devices. We assumed that the emission from the OLED was isotropic, such that the luminance was Lambertian, and calculated the external quantum efficiency from the luminance, current density, and EL spectra.

The optical band gap (E_g) and HOMO position were estimated from the cutoff wavelength of the absorption peak and the spectroscopic measurements of the photoemission in air (AC-3, Rikenkeiki), respectively. We estimated the LUMO position by subtracting E_g from the HOMO position. An absolute PL quantum yield measurement system (C9920, Hamamatsu) and a streak camera (C4334, Hamamatsu) were used to measure the photoluminescence efficiencies (ϕ_{PL}) and transient behaviors of the OLEDs, respectively.

3. Results and discussion

Fig. 1 shows the chemical structures of BDAVBi, DPVBi, Spiro-FA, Spiro-FPA, and MADN, together with the absorption spectrum of BDAVBi in a dilute toluene solution, and the photoluminescence (PL) spectra of thin films of DPVBi, Spiro-FA, Spiro-FPA and MADN. Spiro-FA and Spiro-FPA have excellent thermal properties with T_g values of 110 and 155 °C, respectively. We performed density functional theory (DFT) calculations to characterize the frontier molecular orbital energy levels and three-dimensional geometries of Spiro-FA and Spiro-FPA at the B3LYP/6-31G (d, p) level by using the Gaussian 03 program. The calculated results show that the electron densities of the highest occupied molecular orbital (HOMO) and lowest unoccupied molecular orbital (LUMO) are mostly localized on the anthracene unit in both materials, as shown in Fig. 2. The emission processes can only be attributed to the π–π^* transition centered on the anthracene unit. However, the PL spectrum of the Spiro-FA thin film has a significantly red-shifted, broad emission band, compared with that of the Spiro-FPA thin film. This red shift may be caused by the excimer formation due to the overlap of the anthracene units of adjacent molecules [22,23]. Examples of the molecular packing structure of two adjacent molecules for each host are also shown in Fig. 1, where a part of the anthracene moiety is indicated by a red dashed circle. In a Spiro-FA film, it is possible that several energy states are mixed owing to the overlap of anthracene units between adjacent molecules, which depends on the molecular packing structure [22,23]. On the other hand, the phenyl units in Spiro-FPA, which bind to the anthracene in a direction perpendicular to the anthracene plane, maintain a certain distance between the anthracene units of adjacent molecules. As a result, the excimer formation is suppressed. MADN also has the ideal molecular structure that suppresses the excimer formation [8,19]. We will discuss the effects of the excimer formation of anthracene derivative hosts on the OLED efficiency and the up-conversion of T_1 into S_1 via the TTA process.

The energy diagram of the OLED is shown in Fig. 3. The HOMO/LUMO energies of the four hosts used are determined to be similar. Although the HOMO energy of the guest is smaller than those of the hosts, most of the excitons in OLEDs are formed on the hosts as opposed the to direct trap formation on the guest since the guest concen-

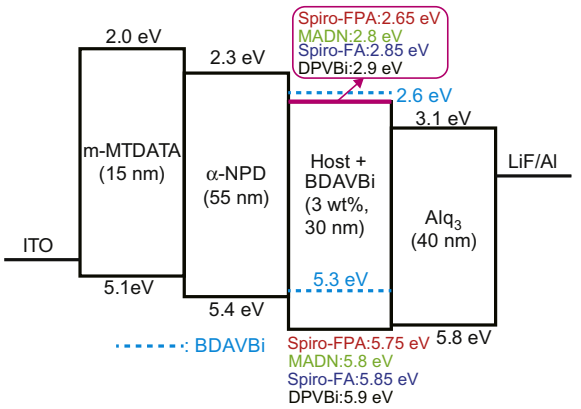

Fig. 3. Schematic energy diagram of devices.

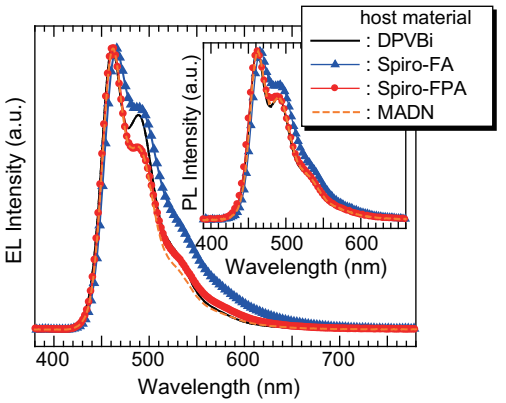

Fig. 4. Electroluminescence spectra of blue OLEDs driven at 1000 cd/m^2. Device configuration is ITO/m-MTDATA/α-NPD/host:BDAVBi (3 wt%)/Alq_3/LiF/Al. Inset: the PL spectra of each emitting layer film. (For interpretation of the references to colour in this figure legend, the reader is referred to the web version of this article.)

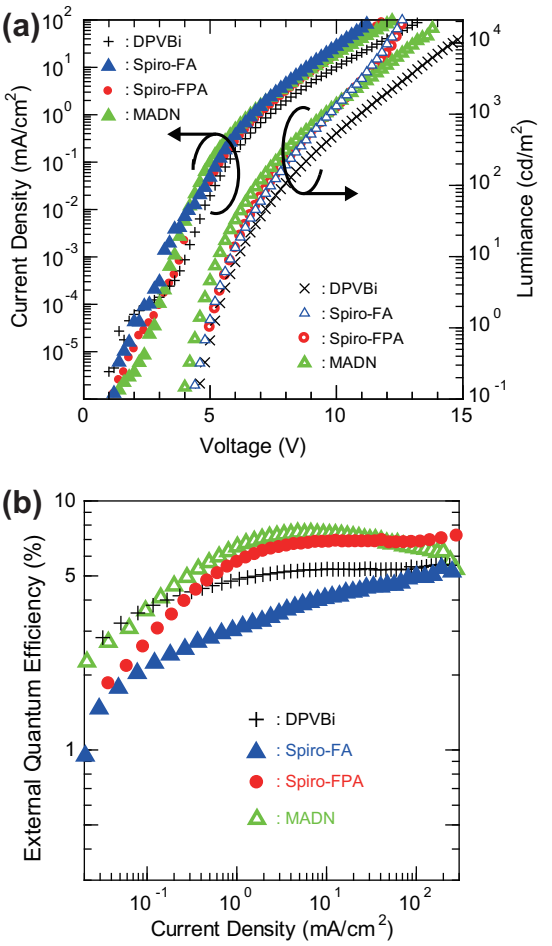

Fig. 5. Current density–voltage–luminance curves (a) and external quantum efficiency-current density curves (b) of BDAVBi-doped blue fluorescent OLEDs. Device configuration is ITO/m-MTDATA/α-NPD/host:BDAVBi (3 wt%)/Alq_3/LiF/Al. (For interpretation of the references to colour in this figure legend, the reader is referred to the web version of this article.)

tration is relatively low (3 wt%) [24]. Actually, the current density–voltage–luminance (*J–V–L*) curves of the OLED, the emitting layer of which is 1 wt% BDAVBi doped MADN, is almost same as that of the OLED using 3 wt% BDAVBi doped MADN as emitting layer (not shown). The EL spectra of the blue OLEDs are shown in Fig. 4. The PL spectra of each emitting layer film are also shown in the inset. We can see from Fig. 4 that there is clearly a difference in onset position between the EL spectrum of the OLEDs and the PL spectrum of each host (Fig. 1). Thus, the observed EL spectra are mainly dominated by the BDAVBi emission caused by the resonant Förster energy transfer of singlet excitons from the host to BDAVBi.

The *J–V–L* curves of the blue OLEDs with different hosts are shown in Fig. 5-(a). We can see from Fig. 5-(a) that the *J–V* characteristics of OLEDs using anthracene derivatives are similar. Thus, the EL spectra and efficiencies of OLEDs using anthracene derivatives are precisely comparable. The device structure of the OLED using DPVBi is optimized to obtain a high η_{ext}; however, the driving voltage of this OLED is higher than those of the other OLEDs. By considering the energy diagram shown in Fig. 3, it is reasonable to suppose that the origin of the difference in driving voltage is the difference in hole/electron mobility between anthracene derivatives and DPVBi. The external quantum efficiency–current density curves of the blue OLEDs are presented in Fig. 5-(b). As shown in Fig. 5-(b), the maximum η_{ext} of the OLED using Spiro-FPA or MADN is higher than that of the OLED using DPVBi. The maximum η_{ext} values of the OLEDs using Spiro-FPA and MADN are more than 7%. When we take the previous reports on blue OLEDs into account [8,13,14,19,20,25], the anthracene derivatives are expected to be useful in developing highly efficient blue OLEDs. On the other hand, the η_{ext} of the OLED using Spiro-FA, which is also an anthracene derivative, has a maximum η_{ext} of about 5%. Despite Spiro-FA and Spiro-FPA having similarity in their molecular structure, there is a significant difference in η_{ext} between the OLED using Spiro-FA and the OLED using Spiro-FPA. In addition, the color purity of the EL spectrum of the OLED using

Spiro-FA is lower than that of the EL spectrum of the OLED using Spiro-FPA, as shown in Fig. 4. Thus, we speculate that not all anthracene derivatives are good hosts for highly efficient blue OLEDs.

Here, we verify the obtained η_{ext} by comparing several architectures as summarized in Table 1. The Commission Internationale de L'Eclairage (CIE) coordinates of the EL spectra of the OLED using each host are also summarized in the Table. The observed difference in the EL spectrum between the OLED using Spiro-FA and the OLED using Spiro-FPA will be discussed later. The η_{ext} is generally represented as:

$$\eta_{ext} = \eta_{int}\eta_{out} = \gamma\eta_r\phi_{PL}\eta_{out} \quad (1)$$

where η_{int} is the internal quantum efficiency, η_{out} is the light-out coupling efficiency, η_r is the fraction of the total excitons formed that result in radiative transitions ($\eta_r \sim 0.25$ for conventional fluorescent molecular dyes), γ is the electron-hole charge-balance factor (assumed to be 1.0), and ϕ_{PL} is the PL quantum efficiency [1]. We measured the ϕ_{PL} values of the undoped and BDAVBi-doped films, and found that ϕ_{PL} is markedly improved by BDAVBi doping in anthracene derivative hosts, as found in Table 1. Evidence of the efficient energy transfer from the anthracene derivatives to BDAVBi can be seen in the spectral overlap between the absorption band of BDAVBi and the emission band of the anthracene derivatives (Fig. 1). The reason why the ϕ_{PL} of the BDAVBi-doped film in DPVBi is higher than that of the other three films is expected to be because of the higher ϕ_{PL} of the host. We can see from Table 1 that the experimental η_{ext} values of the OLEDs using Spiro-FPA and MADN are higher than the calculated η_{ext} from Eq. (1), where η_r and η_{out} are assumed to be 0.25 and 0.2–0.3, respectively. Moreover, the η_r of these OLEDs, estimated from the experimental η_{ext}, ϕ_{PL}, and η_{out}, is higher than the maximum value of 0.25 in conventional fluorescent OLEDs, which implies that TTA contributes to the high efficiency of the OLED using Spiro-FPA or MADN.

To observe the TTA related phenomenon, we examined the transient decay of the electroluminescence by applying an electrical pulse with a width of 100 ns to the OLEDs. It is usually difficult to operate OLEDs by applying an input voltage for a duration of 100 ns [26]. However, we prepared a specialized pulse generator that can apply a voltage of about 35 V with a pulse width of 100 ns [27]. The microsecond range transient phenomena and EL spectrum can be observed by synchronizing the pulse generator with a streak camera in a 500-μs cycle. The transient behaviors of the OLED are shown in Fig. 6-(a). The transient behavior of the OLED using DPVBi shows only a single exponential transient decay, the electroluminescence lifetime (τ) of which is about 100 ns, as indicated by the black arrow. It is likely that the observed τ reflects the pulse width of the pulse generator since the PL lifetime of BDAVBi is about 1 ns. On the other hand, the transient behaviors of the other OLEDs show a second-order transient decay. The

Table 1
PL quantum efficiency (ϕ_{PL}) of each film and performance characteristics of OLEDs. η_{ext} (calc.) represents the upper limit of the external quantum efficiency of the conventional fluorescent OLED based on the classical estimation using four factors. η_r is the fraction of the total excitons formed that result in radiative transitions. The CIE of the EL spectra of the OLED using each host are also shown.

Host	ϕ_{PL} of host film	ϕ_{PL} of BDAVBi doped film (3 wt%)	η_{ext} (calc.) (η_r = 0.25, η_{out} = 0.2–0.3)	Maximum η_{ext} (exp.)	Maximum η_r (exp.) (η_{ext} (exp.)/$\eta_{out}\phi_{PL}$)	CIE (x,y)
DPVBi	0.85	0.86	4.3–6.4%	5.4%	0.20–0.31	(0.15, 0.22)
Spiro-FA	0.33	0.73	3.6–5.5%	5%	0.22–0.34	(0.17, 0.29)
Spiro-FPA	0.35	0.74	3.7–5.6%	7.2%	0.32–0.48	(0.16, 0.23)
MADN	0.37	0.76	3.8–5.7%	7.4%	0.32–0.49	(0.15, 0.22)

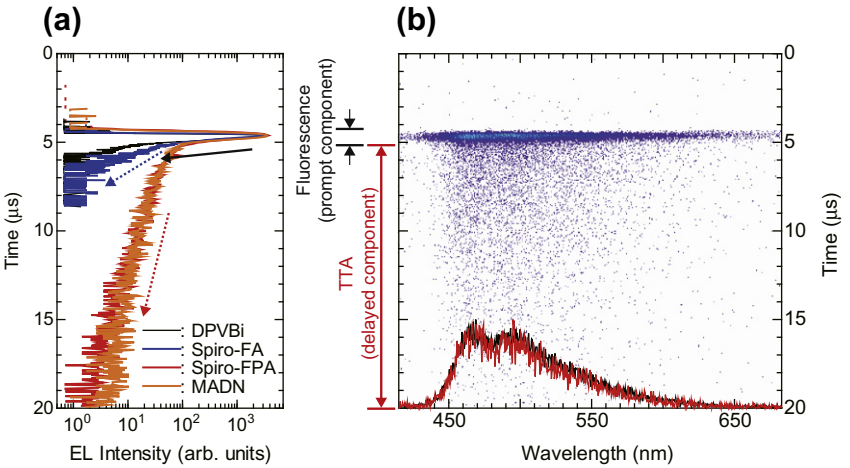

Fig. 6. Transient electroluminescent decay of blue fluorescent OLEDs (a). Streak image and EL spectra of OLED using Spiro-FPA showing prompt component (black) and the delayed component (TTA, red) (b). The spots correspond to the EL intensities of the OLED using spiro-FPA. (For interpretation of the references to colour in this figure legend, the reader is referred to the web version of this article.)

long-lifetime component indicated by the broken line arrow is attributed to the delayed fluorescence caused by the TTA process [13,14]. The contribution of TTA differs depending on the host material. The intensities of the delayed components in the OLEDs using Spiro-FPA and MADN are higher than that in the OLED using Spiro-FA. It is obvious that the observed difference in η_{ext} between the OLEDs using the anthracene derivative hosts is predominantly due to the difference in TTA contribution since ϕ_{PL} is independent of the host materials, as shown in Table 1. Thus, we can conclude that some anthracene derivatives, such as Spiro-FPA and MADN, are suitable hosts for developing highly efficient blue OLEDs utilizing TTA. It is difficult to estimate the contribution of TTA to η_{ext} from the results of the transient behavior in a manner similar to that demonstrated by Kondakov because the pulse width omit differs between this measurement and the reported measurement (~100 μs) [11–14]. In our study, the very short electrical pulse was used to observe both the EL spectra and transient decay in a microsecond range. Fig. 6-(b) presents the streak image of the OLED using Spiro-FPA that corresponds to that in Fig. 6-(a), showing the prompt and delayed EL spectra obtained at 295 K. Because both spectra are nearly coincident, we confirmed that both the prompt and delayed (TTA) components are attributed to the emission of BDAVBi. Some researchers have estimated the contribution of TTA by analyzing delayed fluorescence, on the other hand, this is the first observation of the EL spectra both prompt and delayed fluorescence via TTA [11–14,28].

The principles of the device operations of (a) the OLEDs using Spiro-FPA and MADN and (b) the OLED using Spiro-FA are illustrated in Fig. 7. The principle of device operation of OLED using DPVBi is not shown since it is unrelated to the TTA process and excimer formation. First, we summarize the emission mechanisms of the OLEDs using Spiro-FPA and MADN. The singlet excitons are transferred following a resonant Förster process onto the doped BDAVBi (prompt). In addition, the host triplet excitons up-convert into S_1 via the TTA process, and then the singlet excitons are transferred onto BDAVBi (delayed). We would like to emphasize that the emitting layer should consist of an anthracene derivative host and an efficient dopant for developing efficient blue OLEDs. The anthracene derivatives are effective for the TTA process and the dopants increase ϕ_{PL}. Although the anthracene derivatives show relatively high ϕ_{PL} values, the doping of the guest may be necessary for developing the blue fluorescent OLEDs with η_{ext} values of more than 5%, except in some cases [28–30]. As reported by Yokoyama et al., we suppose that the TTA is independent to host–guest interaction [28]. Next, we discuss the effect of the excimer formation on the efficiency and color purity by summarizing the emission mechanisms of the OLED using Spiro-FA. In the emitting-layer film, several energy states of the host, which depend on the molecular packing structure, are mixed, as shown in Fig. 1. The energy diagrams shown in Fig. 7 are two examples of these energy states. The singlet excitons of the small overlap phase are transferred onto the doped BDAVBi. On the other hand, the singlet energy of the excimer-type phase can be smaller than that of BDAVBi; that is, the singlet excitons are not transferred to the doped BDAVBi [22]. The singlet excitons of the excimer-type phase emit a greenish-blue light, reducing the color purity of the EL spectrum, as shown in Fig. 4 and Table 1. This insufficient energy transfer from Spiro-FA to BDAVBi can also be confirmed from the PL spectra of emitting layer as shown in inset in Fig. 4. It is likely that the triplet excitons of the excimer-type phase cannot up-convert into S_1 since the delayed component in the transient decay is small in the OLED using Spiro-FA, as shown in Fig. 6. Thus, the efficiency of the OLED using Spiro-FA is lower than those of the OLEDs using Spiro-FPA and MADN. The excimer formation should be excluded both to realize a high efficiency and to obtain a pure blue emission. The host material for developing highly efficient blue OLEDs should have an anthracene unit and a bulky molecular structure not only to increase T_g but also to create a steric hindrance that prevents the overlap of anthracene units between adjacent molecules in a film. The reason why the triplet excitons in the excimer-type phase cannot up-convert is supposed to be the difference in the energy arrangement of T_1 and S_1. Although the detailed mechanism of the up-conversion

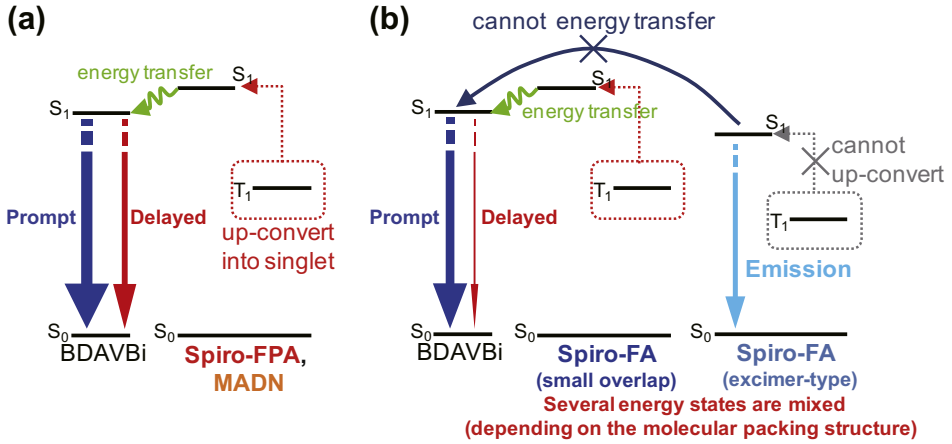

Fig. 7. Schematic representations of emission and/or energy transfer mechanisms in OLEDs using Spiro-FPA and MADN (a) in and OLED using Spiro-FA (b).

is unclear, it is possible that the low triplet energy of anthracene (~1.8 eV) is strongly involved [13,31]. From this point, we are planning an even more detailed examination of the mechanism of the up-conversion of triplet excitons into S_1 via the TTA process.

4. Conclusion

We have presented a detailed comparison of four types of blue OLEDs with respect to the relationship between their host material and their efficiency. The highly efficient blue OLED utilizing triplet–triplet annihilation is developed using a host material with an anthracene unit and a bulky molecular structure. We also found that a bulky molecular structure that prevents the overlap of anthracene units between adjacent molecules in the emitting layer is important for enhancing the up-conversion of triplet excited states into singlet ones. Our results suggest that new molecular design strategies for creating a host material could contribute to realizing more highly efficient blue OLEDs.

References

[1] C. Adachi, M.A. Baldo, M.E. Thompson, S.R. Forrest, J. Appl. Phys. 90 (2001) 5048.
[2] K. Okumoto, H. Kanno, Y. Hamaa, H. Takahashi, K. Shibata, Appl. Phys. Lett. 89 (2006) 063504.
[3] H. Kanno, K. Ishikawa, Y. Nishio, A. Endo, C. Adachi, K. Shibata, Appl. Phys. Lett. 90 (2007) 123509.
[4] S. Watanabe, N. Ide, J. Kido, Jpn. J. Appl. Phys. 46 (2007) 1186.
[5] S.O. Jeon, K.S. Yook, C.W. Joo, J.Y. Lee, K.Y. Ko, J.Y. Park, Y.G. Baek, Appl. Phys. Lett. 93 (2008) 063306.
[6] T.J. Park, W.S. Jeon, J.J. Park, S.Y. Kim, Y.K. Lee, J. Jang, J.H. Kwon, R. Pode, Appl. Phys. Lett. 93 (2008) 113308.
[7] M.S. Weaver, R.C. Kwong, V.A. Adamovich, M. Hack, J.J. Brown, J. Soc. Inf. Disp. 14 (2006) 449.
[8] M.T. Lee, C.H. Liao, C.H. Tsai, C.H. Chen, J. Soc. Inf. Disp. 14 (2006) 61.
[9] J.B. Birks, Photophysics of Organic Molecules, Wiley, New York, 1970. p.372.
[10] B. Valeur, Molecular Fluorescence, Wiley–VCH, Weinheim, 2002. p. 41.
[11] D.Y. Kondakov, T.D. Pawlik, T.K. Hatwar, J.P. Spindler, J. Appl. Phys. 106 (2009) 124510.
[12] C.T. Brown, D. Kondakov, J. Soc. Inf. Disp. 12 (2004) 323.
[13] D.Y. Kondakov, J. Soc. Inf. Disp. 17 (2009) 137.
[14] D.Y. Kondakov, J. Appl. Phys. 102 (2007) 114504.
[15] A. Endo, M. Ogasawara, A. Takahashi, D. Yokoyama, Y. Kato, C. Adachi, Adv. Mater. 21 (2009) 4802.
[16] J.C. Deaton, S.C. Switalski, D.Y. Kondakov, R.H. Young, T.D. Pawlik, D.J. Giesen, S.B. Harkins, A.J.M. Miller, S.F. Mickenberg, J.C. Peters, J. Am. Chem. Soc. 132 (2010) 9499.
[17] A. Endo, K. Sato, K. Yoshimura, T. Kai, A. Kawada, H. Miyazaki, C. Adachi, Appl. Phys. Lett. 98 (2011) 083302.
[18] R. Katoh, K. Suzuki, A. Furube, M. Kotani, K. Tokumaru, J. Phys. Chem. C 113 (2009) 2961.
[19] C.H. Liao, M.T. Lee, C.H. Tsai, C.H. Chen, Appl. Phys. Lett. 86 (2005) 203507.
[20] Y.Y. Lyu, J. Kwak, O. Kwon, S.H. Lee, D. Kim, C. Lee, K. Char, Adv. Mater. 20 (2008) 2720.
[21] W.J. Shen, R. Dodda, C.C. Wu, F.I. Wu, T.H. Liu, H.H. Chen, C.H. Chen, C.F. Shu, Chem. Mater. 16 (2004) 930.
[22] W. Rettig, B. Paeplow, H. Herbst, K. Müllen, J.-P. Desvergne, H. Bouas-Laurent, New J. Chem. 23 (1999) 453.
[23] S. Kera, H. Fukagawa, T. Kataoka, S. Hosoumi, H. Yamane, N. Ueno, Phys. Rev. B 75 (2007) 121305(R).
[24] Y. Sun, N.C. Giebink, H. Kanno, B. Ma, M.E. Thompson, S.R. Forrest, Nature 440 (2006) 908.
[25] K.H. Lee, L.K. Kang, J.Y. Lee, S. Kang, S.O. Jeon, K.S. Yook, J.Y. Lee, S.S. Yoon, Adv. Funct. Mater. 20 (2010) 1345.
[26] Z.Y. Xie, T.C. Wong, L.S. Hung, S.T. Lee, Appl. Phys. Lett. 80 (2002) 1477.
[27] H. Fukagawa, K. Watanabe, S. Tokito, Org. Electron. 10 (2009) 798.
[28] D. Yokoyama, Y. Park, B. Kim, S. Kim, Y. Pu, J. Kido, J. Park, Appl. Phys. Lett. 99 (2011) 123303.
[29] S.K. Kim, B. Yang, Y. Ma, J.H. Lee, J.W. Park, J. Mater. Chem. 17 (2008) 3376.
[30] S.K. Kim, B. Yang, Y.I. Park, Y. Mab, J.Y. Lee, H.J. Kim, J.W. Park, Org. Electron. 10 (2009) 822.
[31] N. Karl, Landort-Bernstein Numerical Data and Fundamental Relationships in Science and Technology, Springer, Germany, 1985. New Series, Vol. 17.